Simulating In-Service Heavy Vehicle Suspension Dynamics

John de Pont, Kailash Thakur, and Mihai Costache
Industrial Research Limited, New Zealand

ABSTRACT

Different heavy vehicle suspensions produce different levels of dynamic wheel loading on pavements and by implication cause different levels for pavement wear for the same static axle load. Clearly suspensions which generate lower wear should be encouraged but this requires some method of assessing suspension performance.

A technique for using a small scale two post servohydraulic shaker facility to replicate in-service suspension behaviour in the laboratory has been developed and tested. In the first stage of this work, suspension displacements were measured during road trials and an iterative procedure was used to determine the shaker excitations needed to generate the same suspension response in the laboratory. The results of these tests have been reported previously.

In this paper, we investigate using simplified dynamic models of the vehicle to relate the pavement profiles generating the in-service behaviour to the shaker excitations which replicate this behaviour in the laboratory. This technique would enable the excitations needed to simulate the on-road behaviour to be generated without having first measured this on-road behaviour. The adequacy of this approach is evaluated and discussed. Differences between suspension performance on the road and in the laboratory are investigated and methods for compensating for these differences are discussed.

INTRODUCTION

The influence of the vertical dynamics of heavy vehicles on pavement wear has been the subject of extensive study in recent years. It is generally accepted that lowering the dynamic loading generated by heavy vehicles will reduce pavement wear although there is still considerable debate on the magnitude of the reduction. The dynamic response of heavy vehicles in motion is complex and thus the problem of assessing the performance of a heavy vehicle/suspension configuration in terms of its impact on pavement wear is not trivial. Over recent years we have been investigating the use of a relatively simple two post servohydraulic facility to replicate, in the laboratory, the on-road dynamic behaviour of a heavy vehicle suspension system (de Pont 1993, 1994) and thus measure the dynamic wheel forces in the laboratory. This work has been reasonably successful but, to date, has required that a road test be undertaken to determine the response of the vehicle's suspension to actual pavement excitations. The software control system for the servohydraulic shakers (which was developed as part of the project) is then used to establish the shaker excitation signals required to generate the same suspension response for the wheels being excited. Once this is achieved the wheel forces can be measured from instrumentation on the shakers. This approach has some limitations. The need for a road test adds to the time and cost involved. It also means that the results are dependent on the test site used. This imposes limitations on the repeatability and transferability of the test. In this paper we investigate using a relatively simple dynamic model of the vehicle to estimate the relationship between the road profiles and the equivalent shaker excitations. This would eliminate the need for road testing and allow the use of a realistic but theoretical road profile or set of profiles which would be stable with time and transferable from test facility to facility.

Numbers of attempts have been made in the past to model the dynamics of the vehicle and references can be made to Cebon (1985), Hunt (1989), Lee and Hedrick (1989), Schiehlen and Schafer (1989) and Venhovens (1994) among others. In this paper we start with the fundamental equations of motion and develop a relatively simple model of the dynamic behaviour of the vehicle which we can calibrate simply through modal analysis testing. This model is then used to estimate the relationships between the vehicle response to on-road excitations and laboratory based shaker excitations.

THE PITCH PLANE MODEL

For the present study a simple pitch plane model as shown in Fig. 1 is used. This model assumes only one spring and one damper at each axle position. Roll behaviour is ignored. This simplification is also used in the laboratory tests where the two post shaker rig used is set up so that each actuator excites a complete axle and so no roll motion is induced. This is justifiable because, except on very rough roads, roll is a negligible contributor to dynamic wheel forces (OECD 1992).
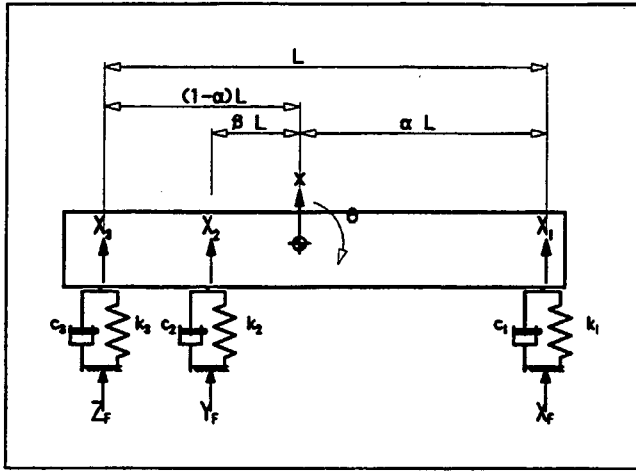
Figure 1. Simple pitch-plane model.

The model also ignores the unsprung mass behaviour of the vehicle. The equations of motion are:

$$m\frac{d^2x}{dt^2}+\sum_{i=1}^{3}(c_i\frac{dX_i}{dt}+k_iX_i)=0 \qquad (1)$$

$$\frac{I}{L}\frac{d^2\theta}{dt^2}+\beta(k_2X_2+c_2\frac{dX_2}{dt})$$
$$+\gamma(k_3X_3+c_3\frac{dX_3}{dt})-\alpha(k_1X_1+c_1\frac{dX_1}{dt})=0 \qquad (2)$$

where the three suspension motions, X_i are related to the whole vehicle motions by

$$X_1 = x - \alpha L\theta - X_F \qquad (3)$$

$$X_2 = x + \beta L\theta - Y_F \qquad (4)$$

$$X_3 = x + \gamma L\theta - Z_F \qquad (5)$$

Figure 1 indicates that the system should have three degrees of freedom. However, EQs (1) and (2) and constraints (3) to (5) restrict the system to only two degrees of freedom. These equations can be solved as shown in appendix A to give the following general solution.

$$y_i(t) = Y_i \exp[(-\xi_i\omega_i + j\omega_i\sqrt{(1 - \xi_i^2)})t] \qquad (6)$$

where the natural frequency of vibration and critical damping ratio are given by

$$\omega_i = \sqrt{\frac{(K_3 + p_iI_rK_2)}{I_rm}} ; \qquad \xi_i = \frac{\lambda\omega_i}{2} \qquad (7)$$

and

$$y_i(t) = L\theta(t) + p_ix(t) \qquad (8)$$

for i = 1, 2 and K_2, K_3 and I_r are as defined in appendix A.

In general both natural modes of vibration are a mixture of bounce and pitch which depend on the geometry of the vehicle. If I_r is less than a critical value the bounce mode is more prominent for the lower frequency and the pitch mode is more prominent for the higher frequency.

The frequencies of the vibrations depend on the values of K_2, K_3, I_r, p_i and m, although these are not all independent. It is interesting to use the model to investigate the effect of load distribution in the vehicle on the natural frequencies and mode shapes. Keeping the total sprung mass constant, it is possible to change the location of the centre of gravity (Cg) of the vehicle and hence change the value of α, β and γ. From EQ (8) we see that when $p_i = 0$ the motion is pure pitch, and that when p_i becomes very large the motion is pure bounce. The variation of p_i with α, (the location of the Cg) is shown in figure 2.
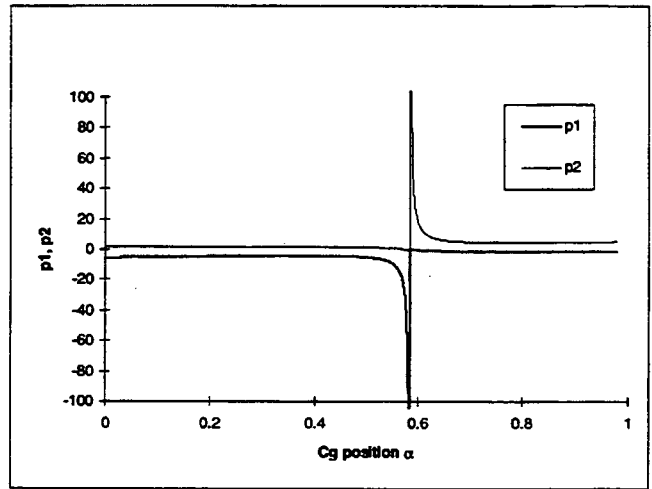

Figure 2. Variation of p_i with Cg position.

The value of p_i becomes either zero or very large near the critical value of α. At this point the modes have separated into pure bounce and pitch. The variation of frequency with α is shown in figure 3.
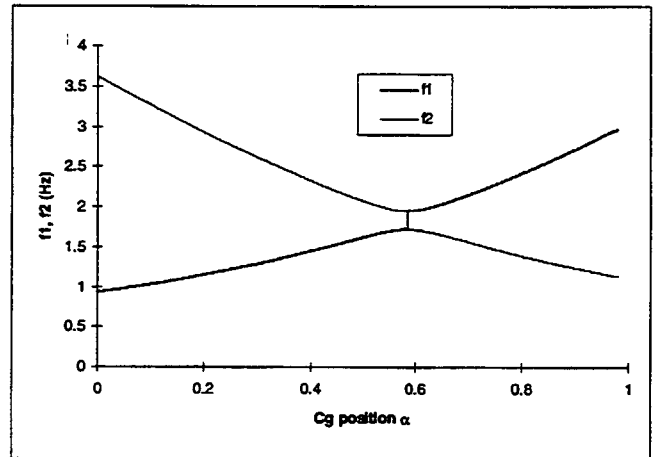

Figure 3. Variation of natural frequencies with Cg position.

The difference between the two natural frequencies becomes minimum at the critical value of α. It is interesting to note that the two normal modes swap over at this transition point. When α is less than the critical values, the first normal mode (i = 1) corresponds to the lower frequency, and the second normal mode (i = 2) corresponds to the higher frequency. When α is greater than the critical value this situation is reversed.

The model's parameters are: mass, pitch inertia, length, axle locations, Cg position and the three stiffness and damping values. Each of the governing EQs (1) and (2) can be divided through by m, the mass, so that the inertia, stiffness and damping terms are all defined as quantities per unit mass. The actual value of the mass is then no longer needed. In the solution in appendix A we have assumed that the damping is proportional to the stiffness for each axle. By weighing the vehicle axle by axle and measuring the axle positions, the mass, and Cg position can be calculated. Using modal testing (Ewins, 1984) the natural frequencies, damping and mode shapes of vehicle can be measured. Appendix B shows how these measurement can be used to calculate the vehicle parameters needed to evaluate the model.

Applying the method now to the three axle tanker trailer fitted with air suspension which has been used in the shaker testing research (de Pont, 1994), we measured and calculated the parameters listed in Table I.

Table 1 Vehicle parameters

Mass (m)	Wheelbase (L)	α	β	γ
19535 kg	5.06m	0.58	0.173	0.42

Using modal testing we found a natural frequency at 1.73 Hz but had great difficulty in finding the other frequency and mode shape we expected with confidence. Eventually we reached the conclusion that, in fact, the two natural frequencies were so close together at 1.73 Hz (effectively both the same) that the modal analysis was not separating them. This requires some modifications to the method for calculating the model parameters. With the two modes effectively superimposed on each other the mode shape results are an arbitrary combination of the two modes and so the procedure (see appendix) for calculating the p_i values could not be applied. However, if we look at EQ (7) we see that if $\omega_1 = \omega_2$ but $p_1 \neq p_2$ then $K_2 = 0$. This implies that

$$\beta k_2 + \gamma k_3 = \alpha k_1 \qquad (9)$$

If we assume that $k_2 = k_3$, that is, that the two axles in the tandem bogey have the same stiffness, we find that $k_1 = 1.02k_2$. EQ (9) is identical in form to the moment balance used to calculate α, β and γ from the axle loads and so the resulting stiffnesses are proportional to the axle loading. As air suspensions are designed to behave in this way this is a perfectly reasonable outcome. As both values of p_i are not zero there is a further condition obtainable from EQ (A15), that is

$$K_3 = I_r K_1 \qquad (10)$$

$$I_r = \frac{\alpha^2 k_1 + \beta^2 k_2 + \gamma^2 k_3}{k_1 + k_2 + k_3}$$

From these and the damping we can calculate all the remaining parameters needed to evaluate the model. These are listed in Table 2.

Table 2 Vehicle dynamics parameters

Inertia ratio (I/mL^2)	k_1/m N/kg.m	k_2/m N/kg.m	k_3/m N/kg.m	c_i/k_i λ
0.182	39.95	39.09	39.09	0.011

When the two modes have identical frequencies the value of α must equal the critical value discussed previously. In this case the values of p_i are indeterminate except that they must satisfy $I_r = -1/p_1 p_2$. However, if we consider a very small shift in α we find the solution $p_1 = -p_2$.

If we estimate the inertia by treating the liquid load as a uniformly distributed mass and the rest of the sprung mass as lumped masses at each of the axles we obtain a value for $I/mL^2 = 0.163$ which is about 11% below the value calculated from the modal tests and the model. If we assume that the spring stiffnesses are 5% lower than those calculated and use this inertia value we obtain two natural frequencies, 1.69 Hz and 1.78 Hz for the two modes. The modal tests we conducted would not have separated two modes as close as this. Thus the results are as consistent as we could reasonably expect. Analysing road test measurements on the same vehicle we also find a single response peak around 1.75 Hz which again supports the model. Hunt (1989) remarked that these two fundamental modes, generally occurring in the frequency range 1.5 Hz to 4 Hz, are often indistinguishable because neither mode is pure bounce or pure pitch. However, our present analysis, the problem of distinguishing the modes occurs because their frequencies are close to each other. Modes that are a combination of bounce and pitch do not present any difficulties for the method.

RESPONSE

Having defined the model we proceed to study the response of the vehicle due to external excitations coming from the road profile through three wheels, ie. X_F (front wheel), Y_F (middle wheel), and Z_F (rear wheel). The equations of motion under the influence of external excitation reduce to

$$\frac{d^2 y_i}{dt^2} + \lambda \omega_i^2 \frac{dy_i}{dt} + \omega_i^2 y_i = \frac{F_i^p(X_F, Y_F, Z_F)}{m} \qquad (11)$$

where

$$F_i^p = p_i F_1 + \frac{mL^2}{I} F_2 \qquad (12)$$

RESPONSE DUE TO ROAD PROFILE

The situation of a vehicle proceeding along a road corresponds to the same excitation disturbance applied to each of the three axles with appropriate time lags which depend on the velocity of the vehicle. Let us consider road excitations of the form

$$X_F = X_F \, e^{j\omega t}$$
$$Y_F = X_F \, e^{j(\omega t + \phi_1)} \qquad (13)$$
$$Z_F = X_F \, e^{j(\omega t + \phi_2)}$$

Let the solution of EQ (11) be of the form

$$y_i(t) = Y_i e^{j(wt + \Phi)} \qquad (14)$$

The response on normal coordinate due to the excitation of the pavement is given by

$$\frac{Y_i e^{j\Phi}}{X_F} = \frac{(1 + j\omega\lambda)[(p_i - \frac{\alpha}{I_r})k_1 + (p_i + \frac{\beta}{I_r})k_2 \, e^{j\phi_1} + (p_i + \frac{\gamma}{I_r})k_3 \, e^{j\phi_2}]}{m([\omega_i^2 - \omega^2] + 2j\omega\omega_i\xi_i)} \qquad (15)$$

The y_i coordinates can be converted to x and θ coordinates using the following equation which is derived from EQ (8)

$$\begin{bmatrix} \dfrac{x}{X_F} \\[2mm] \dfrac{L\theta}{X_F} \end{bmatrix} = \frac{1}{p_1 - p_2} \begin{bmatrix} 1 & -1 \\ -p_2 & p_1 \end{bmatrix} \begin{bmatrix} \dfrac{Y_1 e^{j\Phi_1}}{X_F} \\[2mm] \dfrac{Y_2 e^{j\Phi_2}}{X_F} \end{bmatrix} \qquad (16)$$

These coordinates can in turn be converted to the suspension deflections through EQs (3)-(5) as follows

$$\frac{X_1}{X_F} = \frac{x}{X_F} - \alpha \frac{L\theta}{X_F} - 1$$

$$\frac{X_2}{X_F} = \frac{x}{X_F} + \beta \frac{L\theta}{X_F} - e^{j\phi_1} \qquad (17)$$

$$\frac{X_3}{X_F} = \frac{x}{X_F} + \gamma \frac{L\theta}{X_F} - e^{j\phi_2}$$

SAME EXCITATION ON MIDDLE AND REAR WHEELS WITH TIME DELAY

Now we examine the response of the vehicle in the laboratory situation when the same excitation is applied to the middle and rear wheels with an appropriate time delay. The excitations in this case are

$$X_F = 0, \quad Y_F = Y_F \, e^{j(\omega t + \phi_1)}, \quad Z_F = Y_F \, e^{j(\omega t + \phi_2)} \qquad (18)$$

The response on the normal coordinates due to the above excitations is given by

$$\frac{Y_i e^{j\Phi}}{Y_F} = \frac{(1 + j\omega\lambda)[(p_i + \frac{\beta}{I_r})k_2 \, e^{j\phi_1} + (p_i + \frac{\gamma}{I_r})k_3 \, e^{j\phi_2}]}{m\left[(\omega_i^2 - \omega^2) + 2j\omega\omega_i\xi_i\right]} \qquad (19)$$

The bounce and pitch responses can be obtained from EQs (16) and (19). With this type of laboratory excitation the vehicle response (as calculated from the model) can be matched to the on-road response (as calculated from the model) at only one point on the vehicle. The transfer function needed to convert the road profile excitation to an equivalent laboratory excitation for each of the three possible matches of vehicle response are given below.

(a) Same Response on the front wheel (match X_1 only)

$$\frac{Y_F}{X_F} = \frac{\dfrac{x}{X_F} - \alpha \dfrac{L\theta}{X_F} - 1}{\dfrac{x}{Y_F} - \alpha \dfrac{L\theta}{Y_F}} \qquad (20)$$

(b) Same Response on the middle wheel (match X_2 only)

$$\frac{Y_F}{X_F} = \frac{\dfrac{x}{X_F} + \beta \dfrac{L\theta}{X_F} - e^{j\phi_1}}{\dfrac{x}{Y_F} + \beta \dfrac{L\theta}{Y_F} - e^{j\phi_1}} \qquad (21)$$

(c) Same Response on the rear wheel (match X_3 only)

$$\frac{Y_F}{X_F} = \frac{\dfrac{x}{X_F} + \gamma \dfrac{L\theta}{X_F} - e^{j\phi_2}}{\dfrac{x}{Y_F} + \lambda \dfrac{L\theta}{Y_F} - e^{j\phi_2}} \qquad (22)$$

In each case, the numerator values for x and θ are those calculated from EQ (16) which is a transformation of the results of EQ (15). Those in the denominator are determined by applying the same transformation to the EQ (19) results.

DIFFERENT EXCITATIONS ON THE MIDDLE AND REAR WHEELS

The shaker testing procedure allows two independent excitations to be applied to two axles of the vehicle. The software control system which is called SYSCOMP determines the two excitations required to match a target response at each of the two axles. The target responses used in our tests have been the suspension deflections measured during road tests. In terms of the model, these excitations are written as

$$X_F = 0, \qquad Y_F = Y_F e^{j(\omega t + \phi_1)}, \qquad Z_F = Z_F e^{j(\omega t + \phi_2)} \qquad (23)$$

In this case the suspension displacements at the middle and rear axles are given by

$$\begin{bmatrix} X_2 \\ X_3 \end{bmatrix} = \frac{1}{p_1 - p_2} \begin{bmatrix} 1 & \beta \\ 1 & \gamma \end{bmatrix} \begin{bmatrix} 1 & -1 \\ -p_2 & p_1 \end{bmatrix} \begin{bmatrix} \Psi_1 & \Omega_1 \\ \Psi_2 & \Omega_2 \end{bmatrix} \begin{bmatrix} Y_F \\ Z_F \end{bmatrix} - \begin{bmatrix} Y_F e^{j\phi_1} \\ Z_F e^{j\phi_2} \end{bmatrix} \quad (24)$$

where

$$\Psi_i = \frac{(1 + j\omega\lambda)(p_i + \frac{\beta}{I_r})k_2 \, e^{j\phi_1}}{m\left[(\omega_i^2 - \omega^2) + 2j\omega\omega_i\xi_i\right]}$$

$$\quad (25)$$

$$\Omega_i = \frac{(1 + j\omega\lambda)(p_i + \frac{\gamma}{I_r})k_3 \, e^{j\phi_2}}{m\left[(\omega_i^2 - \omega^2) + 2j\omega\omega_i\xi_i\right]}$$

By equating the suspension response of EQ (24) to that generated by EQs (15), (16), and (17) we can calculate the transfer functions (Y_F/X_F, and Z_F/X_F) required to convert the road profile X_F to the shaker excitations, Y_F and Z_F required to generate the same suspension displacements at the middle and rear axles. Transfer function (Y_F/X_F, and Z_F/X_F) thus computed for our vehicle model are shown in figures 4 and 5.
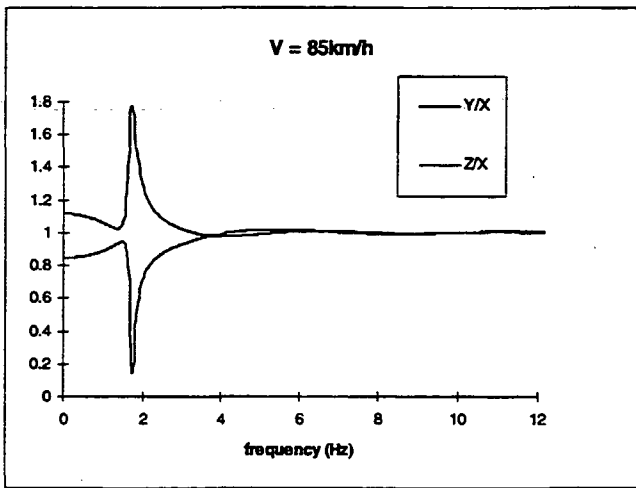

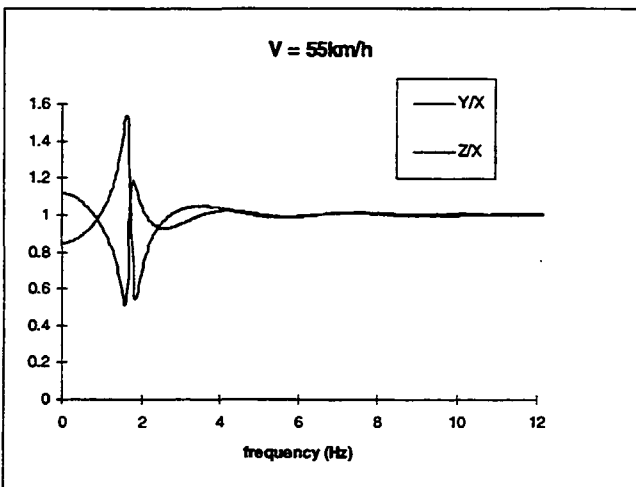Figure 4 Transfer functions for v = 85 km/h

Figure 5 Transfer functions for v = 55 km/h

These functions match the suspension displacement response of the model at middle and rear axles only. There are not sufficient degrees of freedom to match the behaviour at the front axle.

As can be seen these transfer functions are dependent on the vehicle speed. The effect of wheelbase filtering changes significantly with speed. The general pattern is that, at low frequencies, the simulated laboratory excitations are slightly modified versions of the road profile which compensate for the front axle excitation which occurred on the road. At the vehicle modes the compensation required is more complicated and speed dependent and at higher frequencies the transfer functions tend towards unity ie the road profile excitations are applied unchanged.

CALCULATING LABORATORY EXCITATIONS FROM PAVEMENT PROFILES

The transfer functions developed in the previous section can be used to calculate the shaker excitations, Y_F and Z_F (applied at only the middle and rear axles) from measured road profile data, X_F. Figure 6 shows the pavement profiles measured for an urban street in Auckland by the Australian Road Research Board laser profilometer.
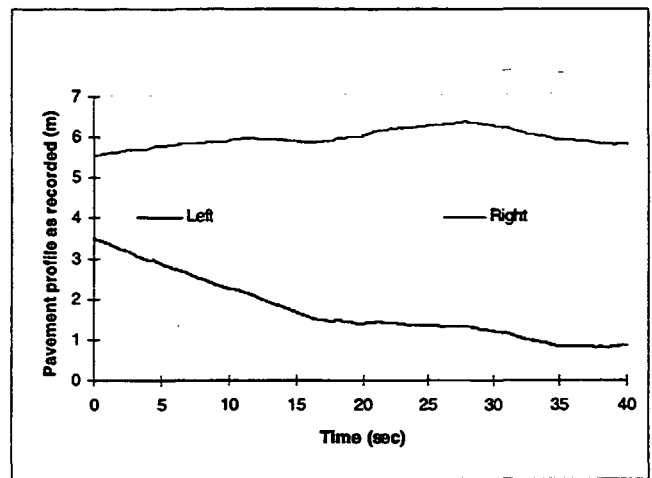

Figure 6. Measured road profiles.

As the profile computation involves the double integration of an accelerometer signal (to compensate for vehicle motions), the output profile has a parabola superimposed over it. As this parabola is of much greater magnitude than the underlying signal it is not easy to filter it out without error. The best method we found was to regression fit a second order polynomial and subtract this from the data. With this approach a good repeatability between repeat measurement set was achieved. Figure 7 shows the processed profiles.

The profile data were recorded at 0.0496465 m intervals. The vehicle measurements were all taken at a sampling rate of 100 Hz. Using the vehicle speed, this time-based sampling rate was converted to equivalent spatial coordinates and the profile data were interpolated to the same coordinate base.
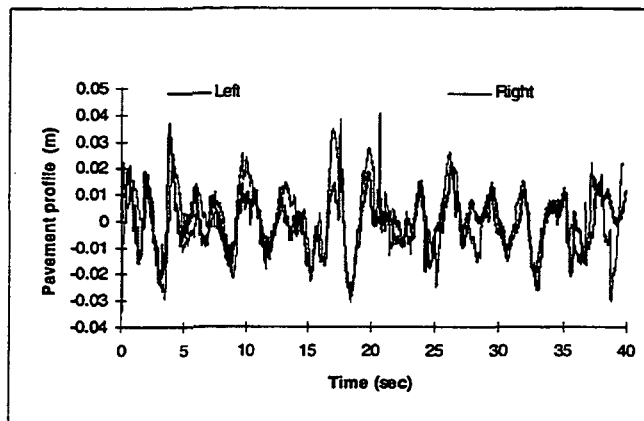
Figure 7. Filtered road profiles.

The resulting pavement profile data, X_F, were converted to equivalent shaker excitations, Y_F and Z_F, using the transfer functions described above. These computed shaker excitation signals are compared with the measurements of those generated by the SYSCOMP software package in matching the measured on-road behaviour of the actual vehicle in figures 8 and 9. The shaker excitations generated by SYSCOMP result in a very good match between the suspension displacements measured in the laboratory and those measured on the road (de Pont, 1994).
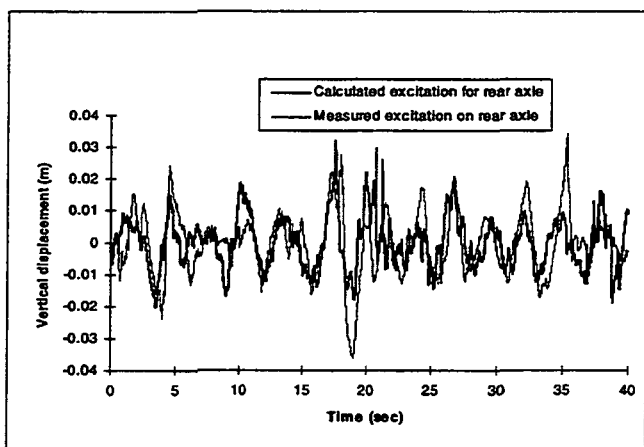

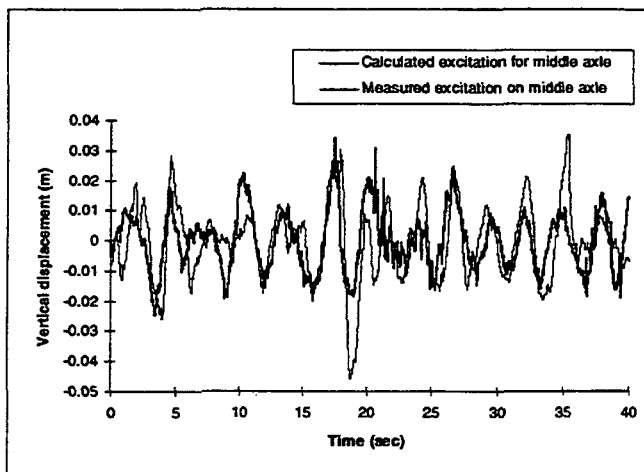Figure 8. Computed vs measured rear excitations.

Figure 9. Computed vs measured middle excitations.

Figures 8 and 9 show that the values of the excitations computed from the road profiles using the model are in reasonably good agreement with those generated by SYSCOMP except for some time shifts at some points. This can be attributed, at least in part, to speed fluctuations during the road test. The profile data were converted to the time domain assuming a constant vehicle speed. Although the tests were nominally undertaken at steady speed some variations are inevitable. A further source of variability is that the measurements of vehicle response and pavement profile were not carried out simultaneously. There was an interval of over a year between these measurements and thus it is likely that some profile changes occurred in this time. Bearing these two factors in mind the match between the calculated excitations and the measured ones is satisfactory.

CALCULATING EXCITATION FROM RESPONSE

EQ (24) can also be used to calculate excitation signals, Y_F and Z_F, from measured response (suspension displacements, X_2 and X_3). These are, of course, the excitations needed to elicit this response from the model and not necessarily those for the actual vehicle. The results of this computation are shown in figures 10 and 11 where they are compared with the laboratory measured displacements.
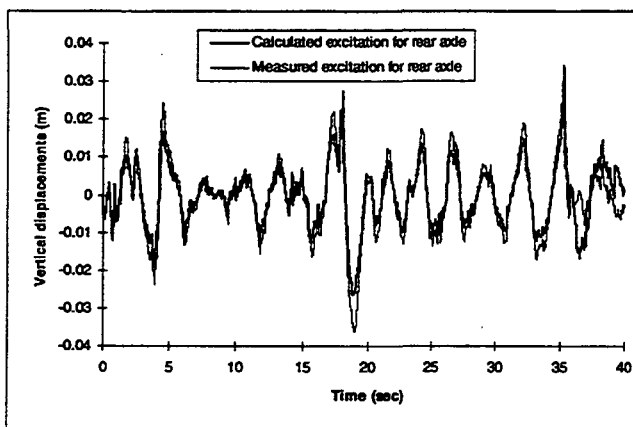

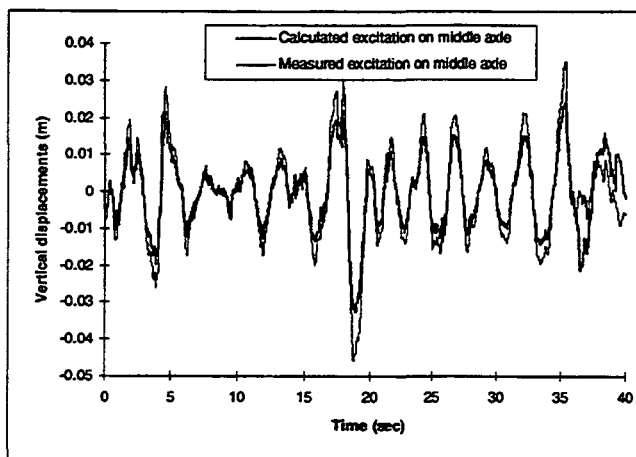Figure 10. Computed vs measured rear excitations.

Figure 11. Computed vs measured middle excitations.

The agreement between computed and exact data is excellent and in fact better than the comparisons in figure 8

and 9. This indicates that the model in fact represents the sprung mass behaviour of the vehicle quite well and that the differences between the excitations calculated from the road profiles and the measured ones may well be caused by errors in the profile rather than inadequacies of the model. It is possible to use this fit between the model response and the actual vehicle response to optimise the values of the model parameters. This is an alternative approach to the modal analysis undertaken previously. If we do this we can recalculate the excitations using the optimised model parameters. The results of doing this are shown in figures 12 and 13.

Table 3 Optimised vehicle dynamics parameters

Inertia ratio (I/mL^2)	k_1/m N/kg.m	k_2/m N/kg.m	k_3/m N/kg.m	c_i/k_i λ
0.140	44.32	43.37	43.37	0.010

Referring back to Table 2, it can be seen that the changes in parameters are small. The spring stiffnesses have increased by about 11% and the inertia ratio is much closer to the value estimated from the vehicle geometry. The damping is virtually unchanged.

HIGHER FREQUENCY MODES

The simplified model described above simulates the sprung mass response of the vehicle and when used to calculate shaker excitations from road profiles only modifies the low frequency components. The higher frequency components of the road profile are unchanged and also part of the shaker excitations. If we consider the typical dynamic behaviour of heavy vehicles we see that this is perfectly reasonable. At higher frequencies the modes of vibration are primarily unsprung mass modes, that is, vibrations of the axle assembly. These will be stimulated by direct excitation at the axle concerned and largely unaffected by inputs at the other axles. For this reason, the excitations required in the laboratory to produce the same behaviour as on the road will be very similar. In terms of the aim of the work which is to be able to assess suspension performance by measuring wheel forces in the laboratory, these higher frequency modes are a significantly smaller contributor to wheel force than the low frequency modes and so it is less critical to reproduce them accurately.
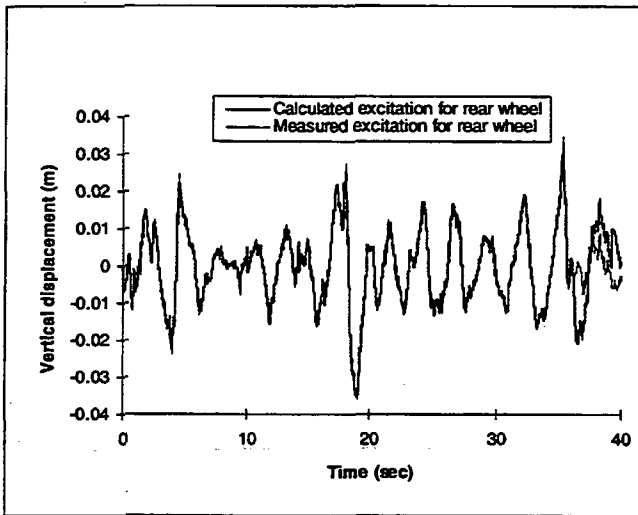

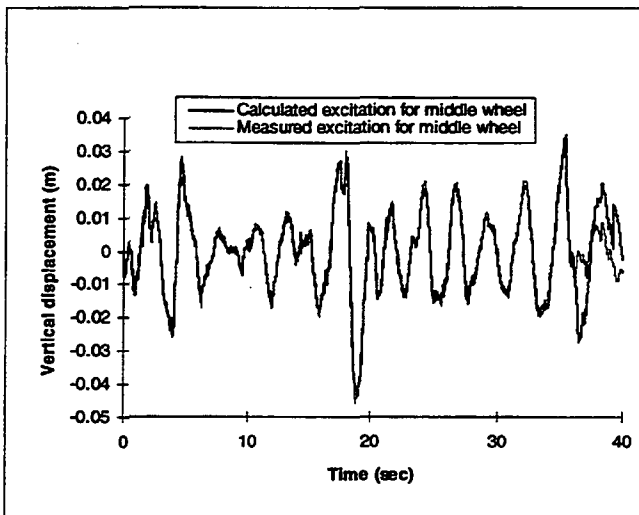Figure 12. Computed vs measured rear excitations

Figure 13. Computed vs measured middle excitations.

The fit is almost perfect. There is a minor discrepancy at the end of the time trace which comes about because the Fourier transform procedure used assumes that the signals are circular which is not correct. The original vehicle response was measured during a test on a straight section of road. There is no reason why the end of the recorded response should match up with the beginning. The optimised model parameters used for this fit are given in Table 3.

CONCLUSIONS

Our aim in this work was to develop a simplified model which behaves sufficiently similarly to the real vehicle to be able to be used for converting the in-service dynamic excitation applied when the three vehicle axles pass over a road profile into a pair of shaker excitations which will produce the same suspension response at the two axles being excited. It was not intended to realistically model the vehicle dynamics in detail.

The model used simulates the sprung mass response of the vehicle and uses linear spring and damper elements. We have developed an algorithm for using modal testing measurements on the vehicle to estimate the model's parameters. The model was then used to calculate the required laboratory excitations from road profile measurements which were compared with those generated by matching the vehicle's measured response. The match obtained was reasonable given that the input road profile data were not ideal. (They were recorded a considerable time before the vehicle response measurements and the conversion to time coordinates using vehicle speed was rather simplified). Using the vehicle response measurements as the input to the excitation calculations gave a significantly improved match. Using the measured response to optimise the model parameters gave an even better result. This

421

suggests a modified modal analysis procedure which uses the shakers excitation and suspension displacement measurements as the response. The next step is to conduct further shaker trials using the calculated excitations as input. The resulting vehicle response can then be compared to the actual response measured during road tests.

Although very simple the model has also provided insights into the interaction of bounce and pitch in the sprung mass response of heavy vehicles and the influence of the position of the Cg and the magnitude of the pitch inertia on the coupling of these modes.

ACKNOWLEDGMENTS

REFERENCES

Cebon, D. (1985) *An Investigation of the Dynamic Interaction Between Wheeled Vehicles and Road Surfaces.* PhD dissertation, University of Cambridge.

de Pont, J.J. (1993) *Rating Heavy Vehicle Suspensions for "Road Friendliness"* Heavy Vehicle Systems, Series B, Int J. of Vehicle Design, Vol.1, No1.

de Pont J.J. (1994) *Experiences with simulating on-road heavy vehicle suspension behaviour using servo-hydraulics.* Engineering Foundation Conference on Dynamic Vehicle/Road and Vehicle/Bridge Interaction. Noordwijkerhout, Netherlands, June 5-10th. To be published in Int J of Vehicle Design.

Ewins, D. J. (1984) *Modal Testing: Theory and Practice.* Research Studies Press, Letchworth, Herts.

Hunt, H. E. M. (1989) *Stochastic Modeling of Vehicles for Calculation of Ground Vibration* in The Dynamics of Vehicles on Road and on Tracks, Proc. 11th IAVSD Symposium, Kingston, Ont., Ed. R. Anderson.

Lee, H.Y. and Hedrick, J.K. (1989) *Dynamic Constraint Equations and their Impact on Active Suspension Performance* in The Dynamics of Vehicles on Road and on tracks, Proc. 11th IAVSD Symposium, Kingston, Ont., Ed. R. Anderson.

OECD (1992) *Dynamic Loading of Pavements,* OECD Road Transport Research, Report prepared by an OECD Scientific Expert Group.

Schiehlen, W. and Schafer, P. (1989) *Modeling of Vehicles with Controlled Components* in The Dynamics of Vehicles on Road and on tracks, Proc. 11th IAVSD Symposium, Kingston, Ont., Ed. R. Anderson.

Venhovens, P. J. Th. (1994). *The Development and Implementation of Adaptive Semi-Active Suspension Control,* Vehicle System Dynamics, 23, 211-35.

APPENDIX A

SOLUTION OF EQUATIONS OF MOTION OF MODEL

The equations of motion are:

$$m\frac{d^2x}{dt^2} + \sum_{i=1}^{3}(k_i X_i + c_i \frac{dX_i}{dt}) = 0 \qquad (A1)$$

and

$$\frac{I}{L}\frac{d^2\theta}{dt^2} + (k_2 X_2 + c_2\frac{dX_2}{dt})\beta \\ + (k_3 X_3 + c_3\frac{dX_3}{dt})\gamma - (k_1 X_1 + c_1\frac{dX_1}{dt})\alpha = 0 \qquad (A2)$$

where the three suspension motions, X_i are related to the whole vehicle motions by

$$X_1 = x - \alpha L\theta - X_F \qquad (A3)$$

$$X_2 = x + \beta L\theta - Y_F \qquad (A4)$$

$$X_3 = x + \gamma L\theta - Z_F \qquad (A5)$$

Although there are three suspension movements equations (A3) to (A5) constrain them to each other so that the system has only two degrees of freedom. Substituting EQs (A3) to (A5) into EQs (A1) and (A2) gives us the following two equation in two variables.

$$m\frac{d^2x}{dt^2} + (c_1 + c_2 + c_3)\frac{dx}{dt} \\ + (c_2\beta + c_3\gamma - c_1\alpha)L\frac{d\theta}{dt} \\ + (k_1 + k_2 + k_3)x \\ + (k_2\beta + k_3\gamma - k_1\alpha)L\theta = F_1 \qquad (A6)$$

and

$$\frac{I}{L}\frac{d^2\theta}{dt^2} + (\alpha^2 c_1 + \beta^2 c_2 + \gamma^2 c_3)L\frac{d\theta}{dt} \\ + (\beta c_2 + \gamma c_3 - \alpha c_1)\frac{dx}{dt} \\ + (\alpha^2 k_1 + \beta^2 k_2 + \gamma^2 k_3)L\theta \\ + (\beta k_2 + \gamma k_3 - \alpha k_1)x = F_2 \qquad (A7)$$

where

$$F_1 = c_1\frac{dX_F}{dt} + c_2\frac{dY_F}{dt} + c_3\frac{dZ_F}{dt} \\ + k_1 X_F + k_2 Y_F + k_3 Z_F$$

$$F_2 = \beta k_2 Y_F + \gamma k_3 Z_F - \alpha k_1 X_F \\ + \beta c_2\frac{dY_F}{dt} + \gamma c_3\frac{dZ_F}{dt} - \alpha c_1\frac{dX_F}{dt}$$

In order to determine the normal modes of vibration and the natural frequencies, we set the excitations to zero, i.e. $F_1 = F_2 = 0$.

If we restrict the solution to the case where,

$$\frac{k_1}{c_1} = \frac{k_2}{c_2} = \frac{k_3}{c_3} = \frac{1}{\lambda} \qquad (A8)$$

Then we can make the following substitutions in our equations of motion,

$$k_1 + k_2 + k_3 = K_1 \\ (\gamma k_3 + \beta k_2 - \alpha k_1) = K_2 \\ (\alpha^2 k_1 + \beta^2 k_2 + \gamma^2 k_3) = K_3 \qquad (A9) \\ \frac{mL^2}{I} = \frac{1}{I_r}$$

Hence, EQs (A6) and (A7) reduce to

$$m\frac{d^2x}{dt^2} + K_2(\lambda L\frac{d\theta}{dt} + L\theta) + K_1(\lambda\frac{dx}{dt} + x) = 0 \quad (A10)$$

and

$$mL\frac{d^2\theta}{dt^2} + \frac{K_2}{I_r}(\lambda\frac{dx}{dt} + x) + \frac{K_3}{I_r}(\lambda L\frac{d\theta}{dt} + L\theta) = 0 \quad (A11)$$

We can arbitrarily create a new variable y(t) which is a linear combination of the existing variables, $\theta(t)$ and x(t) as follows,

$$y(t) = L\theta(t) + px(t) \qquad (A12)$$

where p is an arbitrary constant.

Combining equations p. EQ(A10) + EQ(A11), we obtain

$$m\frac{d^2y}{dt^2} + \lambda p\frac{dx}{dt}(\frac{K_2}{I_r p} + K_1) + \lambda L\frac{d\theta}{dt}(\frac{K_3}{I_r} + K_2 p) \\ + px(\frac{K_2}{I_r p} + K_1) + L\theta(\frac{K_3}{I_r} + K_2 p) = 0 \qquad (A13)$$

If we choose p so that

$$\frac{K_2}{I_r p} + K_1 = K_2 p + \frac{K_3}{I_r} \qquad (A14)$$

i.e. p satisfies the quadratic equation

$$p^2 I_r K_2 + p(K_3 - K_1 I_r) - K_2 = 0 \qquad (A15)$$

There are two real values of p (p_i, i = 1, 2) which satisfy this condition and hence EQ (A13) becomes two equations of the form,

$$m\frac{d^2y}{dt^2} + \lambda(\frac{K_3}{I_r} + p_iK_2)\frac{dy}{dt} + (\frac{K_3}{I_r} + p_iK_2)y = 0 \quad \text{(A16)}$$

These can be solved for the two normal modes of vibration as given by EQ (A17).

$$y_i(t) = Y_i \exp[\{-\xi_i\omega_i + j\omega_i\sqrt{(1 - \xi_i^2)}\}t] \quad \text{(A17)}$$

The natural frequency of vibration and critical damping ratio are given by

$$\omega_i = \sqrt{\frac{(K_3 + p_iI_rK_2)}{I_rm}}; \quad \xi_i = \frac{\lambda\omega_i}{2} \quad \text{(A18)}$$

with $i = 1, 2$.

APPENDIX B

EVALUATING MODEL PARAMETER FROM MODAL TEST MEASUREMENTS.

Consider now how the model parameters might be determined. If the axle loads and spacings are measured, it is a simple matter to calculate the mass and the position of the Cg for the whole vehicle. As the motion we are modeling is that of the sprung mass, it is better to first estimate the unsprung mass of each axle and subtract this from the axle loads measured before calculating the Cg position. For the three axle trailer we are using this has virtually no effect on the result. Thus we have parameters, m, L, α, β and γ. If we then undertake a modal analysis on the vehicle we can measure the frequency, damping and mode shapes of the two fundamental modes of vibration. The mode shapes are measured in terms of the motions of the ends of the vehicle, variables X_1 and X_2 (as defined in EQs (A3) and (A5)). From EQs (A3), (A5) and (A12), X_1 and X_3 can be related back to the modal variables y_i.

$$\begin{bmatrix} y_1 \\ y_2 \end{bmatrix} = \begin{bmatrix} \gamma p_1 - 1 & \alpha p_1 + 1 \\ \lambda p_2 - 1 & \alpha p_2 + 1 \end{bmatrix} \begin{bmatrix} X_1 \\ X_3 \end{bmatrix} \quad \text{(B1)}$$

In the modal coordinate system, y_i, the eigenvectors are (1,0) and (0,1). Thus we can use EQ (A19) to solve for the p_i values from the mode shapes as measured in X_1, X_3 coordinates. From EQ (A15) constraining the p values we can show that

$$I_r = -\frac{1}{p_1p_2} \quad \text{(B2)}$$

From EQs (A18) and (A14) we can show that

$$K_1 = \frac{m(p_2\omega_2^2 - p_1\omega_1^2)}{p_2 - p_1}$$

$$K_2 = \frac{m(\omega_2^2 - \omega_1^2)}{p_2 - p_1} \quad \text{(B3)}$$

$$K_3 = \frac{mI_r(p_2\omega_1^2 - p_1\omega_2^2)}{(p_2 - p_1)}$$

which from EQ (A9) is a linear system of three equations in three unknowns, k_1, k_2 and k_3 which can be solved.

From the modal damping and EQ (A18) we can calculate λ. Thus all the parameters in the model have been determined.